 https://dx.doi.org/10.1109/IGARSS52108.2023.10282493

A CONTROLLED GROUND-BASED EXPERIMENT TO ASSESS THE CAPABILITIES OF GNSS-R FOR MARINE LITTER DETECTION IN A FLUME

A. Gonga[1, 2], A. Perez-Portero[1, 2], A. Camps[1, 2, 3], D. Pascual[4], A. de Fockert[5], and P. de Maagt[6]

[1]CommSensLab – UPC, Universitat Politècnica de Catalunya – BarcelonaTech, Barcelona, Spain
[2]Institute of Space Studies of Catalonia (IEEC) – CTE-UPC, E-08034 Barcelona, Spain
[3]ASPIRE Visiting International Professor, UAE University, CoE, POBox 15551 Al-Ain, UAE
[4]DEIMOS Space UK Ltd., AIRSPEED 1, 151 Eighth St, Harwell Oxford, Didcot OX11 0RL, UK
[5]Boussinesqweg 1, 2629 HV Delft, NL
[6]European Space Research and Technology Centre (ESTEC), Keplerlaan 1, 2201 AZ Noordwijk, NL

ABSTRACT

Detection of marine litter is an urgent task given the large amount of plastics that end up in all water systems. This manuscript provides the description and results obtained from a ground-based Global Navigation Satellite System - Reflectometry (GNSS-R) system built in a controlled indoor environment intended to test the capabilities of GNSS-R techniques for marine litter detection, when different wave conditions and plastic litter were used. Results show that it may be possible to detect the damping of waves produced by the accumulations of some types of plastic.

Index Terms— GNSS-R, Marine litter, Polarization, Remote Sensing

1. INTRODUCTION

Some works have recently reported the potential of GNSS-R to detect marine litter from space [1]. The main hypothesis relies on the fact that the presence of plastics damps large waves, and this damping effect is even increased by the presence of biofouling on the plastic's surfaces [2].

As part of the Global Monitoring of Microplastics using GNSS-Reflectometry (GLIMPS) project led by Deimos Space UK, the Polytechnic University of Catalonia (UPC) conducted a ground-based GNSS-R experiment in a controlled water flume: the "Atlantic Basin" at Deltares' research premises (Delft, NL).

The main objective was the assessment of how different plastics sizes could produce a detectable effect through a change in the surface roughness either by damping the waves, or by creating new capillary waves produced by the distortion of the wavefronts by the presence of plastics.

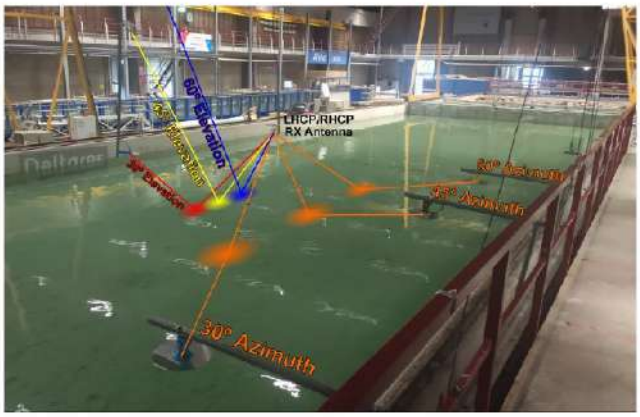

Fig. 1. GNSS-R system built at Deltares. In the middle of the Atlantic basin the elevation transmitters and receivers are hanging, while in the lateral side the azimuthal transmitters are located. The 60° elevation antenna is not shown. (from [3])

2. GROUND-BASED GNSS-R-LIKE SYSTEM DESCRIPTION

2.1. Transmission System

By means of a Rhode & Schwarz vector signal generator (SMU-200A), a synthetic GPS-like signal at L1-band ($f = 1575.42$ MHz) was recorded and played back by using an ADALM-PLUTO (rev B), a Commercial of-the-shelf (COTS) Software Defined Radio (SDR) from Analog Devices. The signal included the Coarse/Acquisition (C/A) Pseudo-Random Noise (PRN) codes from Space Vehicles (SV) 16, 20, 29, and 31 simultaneously, with a power level of -81 dBm. Short coherent integration times (i.e. $T_{coh} = 1$ ms, without incoherent averaging) were measured thanks to such a high Signal-to-Noise Ration (SNR). Moreover, at the beginning and at the end of the GPS-like signal, a continuous wave

beacon centred at L1-band + 500 kHz was also transmitted to track any frequency offsets and drifts.

The system was capable to sweep between different transmitters located at specific distances and heights to mimic different incidence angles of the transmitted signal w.r.t waves propagation. This was in order to assess whether it exists a direct relation in the detection of plastics (Fig. 1). Thus, 3 out of the 6 transmitting antennas where at elevation angles of 60°, 45°, and 30° for 0° azimuth, meanwhile the other 3 where at azimuthal angles of 60°, 45°, and 30° for 30° elevation. All of them were down-looking oriented with Right Hand Circular Polarization (RHCP).

A Radio-Frequency (RF) switching matrix controlled by a Raspberry Pi was used to perform the sequential sweep of the transmitting antennas. Moreover, the RF signal was conditioned by means of a variable attenuator and a fixed amplifier for the signal path losses compensation from each antenna.

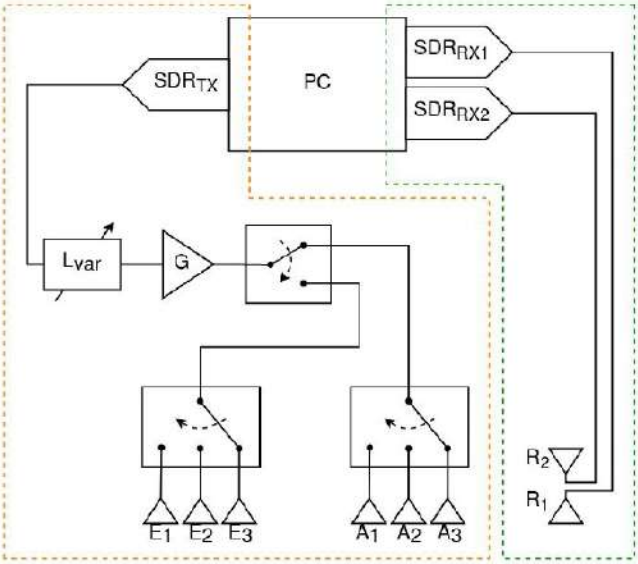

Fig. 2. Block diagram with the transmitter (orange) and the receiver (green) parts of the GNSS-R-like system developed for the GLIMPS experiment at Deltares. (from [3])

2.2. Reception System

The signal being transmitted sequentially by each transmitting antenna was then received simultaneously by two antennas placed at 1 m height w.r.t water level. One being up-looking oriented was in charge of gathering the direct signal at RHCP, meanwhile the second one down-looking oriented was in charge of acquiring the signal scattered on the water surface at dual polarization; Left Hand Circular Polarization (LHCP) and RHCP.

The up-looking antenna was connected to a Universal Software Radio Peripherial (USRP) model B200mini-i from Ettus Research. This was able to down-convert and sample the signal at a rate of $f_s = 2.5$ MSps, signal used as the reference one. On the other hand, the down-looking antenna was connected to an ADALM-PLUTO (rev C) SDR for the signal down-conversion and sampling at $f_s = 2.048$ MSps for both polarizations.

2.3. Reflection Geometry

- Elevation antennas:
  As it can be seen in Fig. 3, the longitudinal separation between the masts holding the transmitting and receiving antennas was 3.46 m. Since the receiving antennas were at 1 m height, the height of the elevation antennas to achieve 30°, 45°, and 60° reflection angles were 1.00 m, 2.46 m, and 5.00 m, respectively.

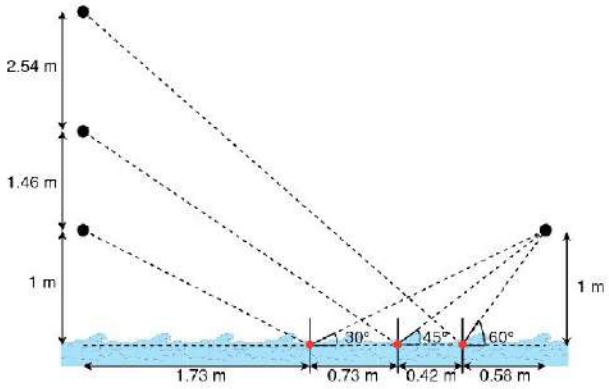

Fig. 3. Sketch of the elevation antennas geometry ("Atlantic Basin" side view). Black dots correspond to the antennas, and red dots the specular reflection points.

- Azimuthal antennas:
  From Fig. 4 it can be seen that the transversal distance between the transmitting and receiving antennas was 4.35 m. To achieve azimuthal angles of 30°, 45°, and 60°, the longitudinal separation of the transmitters were 7.52 m, 4.34 m, and 2.50 m, respectively.

Because of the small distances involved, a strong coherent component is expected. When a coherent reflection occurs, the area from which the signals are coming from is given by the so-called "first Fresnel zone". The first Fresnel zone is the ellipsoidal area surrounding the specular point where the path difference with respect the specular point is less than half wavelength ($\Delta r \leqslant \lambda/2$), or less than a phase shift of $\Delta\phi \leqslant 180°$:

$$R_1 = \frac{\sqrt{\lambda \cdot \frac{D_{10} \cdot D_{20}}{D_{10}+D_{20}}}}{\cos\theta_i}, \tag{1}$$

where:

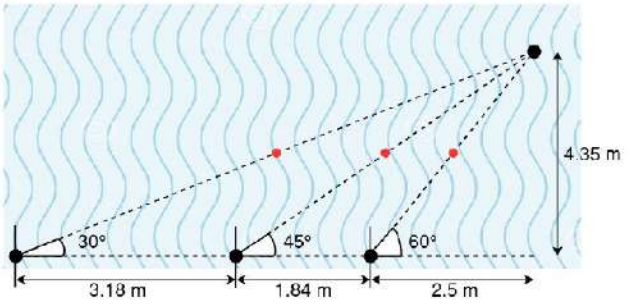

Fig. 4. Sketch of the azimuthal antennas geometry ("Atlantic Basin" top view). Black dots correspond to the antennas, and red dots the specular reflection points.

R_1 is the first Fresnel zone radius,
λ is the electromagnetic wavelength,
D_{10} is the transmitter - specular point distance,
D_{20} is the receiver - specular point distance,
θ_i is the local incidence angle.

From the distances between the transmitters and the receivers, the radii of the first Fresnel zone are calculated and shown in Table 1. (from [3])

Table 1. First Fresnel zones specifications of the GNSS-R-like system built at Deltares.

	Angle [°]	D_{10} [m]	D_{20} [m]	R_1 [m]
Elevation	30	2.00	2.00	0.87
	45	3.48	1.41	0.62
	60	5.77	1.16	0.49
Azimuth	30	5.02	5.02	1.38
	45	3.55	3.55	1.16
	60	2.90	2.90	1.05

2.4. Measurement Conditions

2.4.1. Generated Waves

Two different waves spectra were generated, regular waves describing a sinusoidal shape with a fundamental frequency of 0.833 Hz, and irregular waves with a JONSWAP spectrum [4]. Four different amplitudes were generated (5, 9, 12, and 17 cm), and in selected cases, capillary waves were also generated on top of the long waves by means of a fan as they are weaker and easier to be damped.

2.4.2. Plastic Litter

Plastics of different shapes, sizes, and types were used at different concentrations to assess its impact over the GNSS-R observables while flowing under the first Fresnel zone. The plastics used were:

1. Water bottles
2. Bottle caps and lids
3. Fishing nets
4. Marine litter bags
5. Styrofoam
6. Straws
7. Polyethylene and polypropylene pellets

3. DISCUSSION OF THE OBTAINED RESULTS

As mentioned before, the high SNR allowed to use a coherent integration time of $T_{coh} = 1$ ms without incoherent averaging for the correlation of the GPS signals. Relative calibration for each recorded scenario using the calm water surface as reference was performed. Since most of the changes induced by the presence of marine litter were very small, a statistical analysis was performed from the signal amplitude power and phase. The following amplitude power and phase of the received signal were analysed: time series, TX RHCP - RX RHCP and TX RHCP - RX LHCP (RR and RL from now on) scatter, spectra, and histogram (Fig. 5).

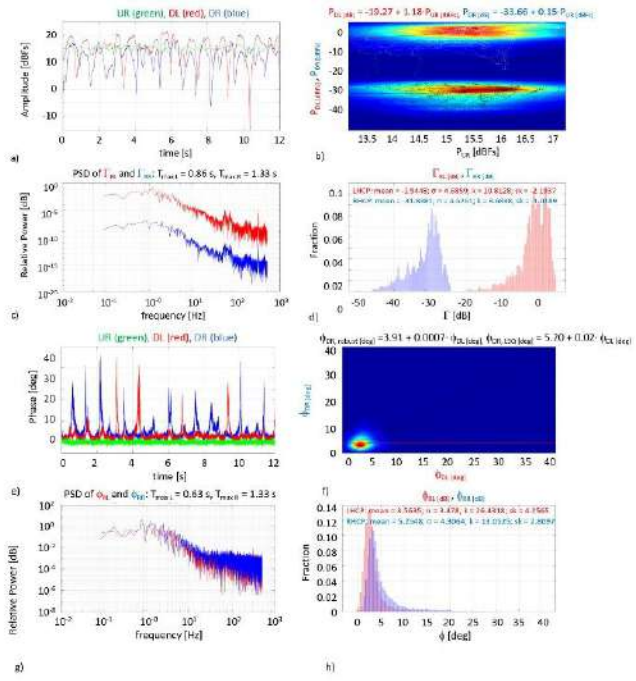

Fig. 5. Clean roughed water surface (5 cm wave height) without capillary waves (TX: 30° el, 0° az).

Because of the GNSS-R-like system was built in an indoor controlled basin, some scenarios had to be discarded due to the presence of Radio-Frequency Interference (RFI) or even Electromagnetic Interference (EMI) probably coming from power lines.

Time series (Fig. 5a, e) provides an insight of the power

Table 2. Summary table of sensitivities for most "promising observables" to detect marine plastic litter. Color indicates: green = possible, orange = difficult, red = very difficult, and black = marginal.

Scenario	Amplitude	Phase
1. Clean water (from flat to rough surface)	- Surface roughness ↑ ⇒ $\sigma(\Delta\Gamma_{RL})$ ~ -9 dB - Capillary waves ↑ ⇒ $\sigma(\Delta\Gamma_{RL})$ ~ - 1-1.5 dB - Kurt varies in both cases	- Sharp decrease $\sigma_{\angle\lvert\Gamma_{RL}\rvert}$ with increasing rms height and presence of capillary waves - Kurtosis and Skewness: ↑ long waves, ↑↑ long and capillary waves
2. Clean water (sinusoidal vs Jonswap)	- Different temporal behavior - $\sigma(\Gamma_{RL\ JONSWAP}) < \sigma(\Gamma_{RL\ sinusoidal})$ by ~0.2-0.4 dB	- $\sigma_{\angle\lvert\Gamma_{RL}\rvert}$ smaller for sinusoidal - No clear trend
3. Bottles and fixed net	- $\sigma(\Delta\Gamma_{RL})$ ↑ ~ 2.5-3 dB with net and bottles, ~ 0.4 dB with net only - Kurtosis ↑	- $\sigma_{\angle\lvert\Gamma_{RL}\rvert}$ ↑ 0.6°- 0.8° - Marginal effect on other observables
4. Straws	- $\sigma(\Delta\Gamma_{RL})$ ↓ by ~ 2-2.5 dB @ 30°, (!!??) ↑ by ~ 0.8 dB @ 60°	- $\sigma_{\angle\lvert\Gamma_{RL}\rvert}$ ↑: 0.7-0.8 °
5. Pellets	- $\sigma(\Delta\Gamma_{RL})$ ↑ ~0.8-1.2 dB @ 30° and 45° - Kurtosis ↑ ~2 @ 30° and 45°	- $\sigma_{\angle\lvert\Gamma_{RL}\rvert}$ ↑ by ~0.2° and ~1.1° @30° and 45°, ↓ by ~4.5° @ 60°
6. Bottles	- $\sigma(\Delta\Gamma_{RL})$: ↑ by 0.8 dB	- Marginal
7. Marine litter (food wraps and bags)	- $\sigma(\Delta\Gamma_{RL})$: ↓ by 0.8 dB at 5 cm rms ↑ by 1.8 dB at 9 cm rms ↓ by 0.4 dB at 17 cm rms - Capillary waves damp increase of reflectivity fluctuations	- $\sigma_{\angle\lvert\Gamma_{RL}\rvert}$ ↓ by ~1.4° @ 5 cm rms, ↑ by ~1.1° @ 9 cm rms and ↓ by ~0.3° @ 17 cm rms
8. Marine litter (nets)	- $\sigma(\Delta\Gamma_{RL})$: ↑ by 1.4 dB	- $\sigma_{\angle\lvert\Gamma_{RL}\rvert}$ ↑: 1.6° @ 30°
9. Styrofoam	- $\sigma(\Delta\Gamma_{RL})$: ↑ by 0.7 dB	- $\sigma_{\angle\lvert\Gamma_{RL}\rvert}$ ↑: 0.5° @ 30° (marginal)
10. Caps and lids	- $\sigma(\Delta\Gamma_{RL})$: ↑ by 0.4 dB Capillary waves damp increase of reflectivity fluctuations	- $\sigma_{\angle\lvert\Gamma_{RL}\rvert}$ ↑: 0.9° @ 30° 1.7° if capillary waves
11. Nets	- $\sigma(\Delta\Gamma_{RL})$: ↑ by 0.6 dB	- $\sigma_{\angle\lvert\Gamma_{RL}\rvert}$ ↑: 0.3° @ 30° (marginal)

and phase variations, correlated with the wave profile on each scenario. RR and RL power scatter plot (Fig. 5b) allowed to discard data with RFI whenever the variation of the direct signal (horizontal axis) was large. Mean value, standard deviation, kurtosis, and skewness statistical descriptors were obtained for the amplitude and phase (Fig. 5d, h).

Table 2 summarizes the sensitivities of the reflectivity amplitude and phase for the different studied cases. It can be seen that the scenarios with a higher impact in the GNSS-R observables had been the bottles attached to a fixed net, food wraps and bags, and nets. The interested reader is invited to read a more detailed analysis that can be found in [3].

4. CONCLUSIONS

This article has described the experimental set-up and processing results obtained during the experiment conducted by UPC at the Deltares "Atlantic Basin" as part of the GLIMPS project led by DEIMOS UK for ESA.

Under the experimental conditions presented, the types of marine litter that can possibly be detected are bottles and fixed nets, food wraps and bags, and nets, as they are the ones that dampen the most the long waves of the water surface.

5. ACKNOWLEDGEMENTS

This article was part of the project "GENESIS: GNSS Environmental and Societal Missions – Subproject UPC", Grant PID2021-126436OB-C21 funded by the Ministerio de Ciencia e Investigación (MCIN)/Agencia Estatal de Investigación (AEI)/10.13039/501100011033 and EU FEDER "Una manera de hacer Europa".

Amadeu Gonga (FI2022/809) and Adrian Perez-Portero (FISDUR2020/105) were supported by grants for recruitment of early-stage research funded by the Agència Gestió d'Ajuts Universitaris i de Recerca (AGAUR) Generalitat de Catalunya, Spain.

6. REFERENCES

[1] M. C. Evans and C. S. Ruf, "Toward the Detection and Imaging of Ocean Microplastics With a Spaceborne Radar," *IEEE Transactions on Geoscience and Remote Sensing*, vol. 60, pp. 1–9, 2022.

[2] N. Rodriguez-Alvarez and K. Oudrhiri, "The Bistatic Radar as an Effective Tool for Detecting and Monitoring the Presence of Phytoplankton on the Ocean Surface," *Remote Sensing*, vol. 13, no. 12, pp. 2248, jun 2021.

[3] A. Gonga, A. Perez-Portero, A. Camps, D. Pascual, A. de Fockert, and P de Maagt, "GNSS-R Observations of Marine Plastic Litter in a Water Flume: An Experimental Study," *Remote Sensing*, vol. 15, no. 3, pp. 637, jan 2023.

[4] K. Hasselmann, T. Barnett, et al., "Measurements of wind-wave growth and swell decay during the Joint North Sea Wave Project (JONSWAP)," *Deut. Hydrogr. Z.*, vol. 8, pp. 1–95, 01 1973.